

Raman scattering properties of human pterygium tissue

Aiguo Shen

Yong Ye

Xiaohua Wang

Changchun Chen

Wuhan University
College of Chemistry and Molecular Sciences
Wuhan, 430072, China

Hanbin Zhang

Wuhan AIER Eye Hospital
Wuhan, 430063, China

Jiming Hu

Wuhan University
College of Chemistry and Molecular Sciences
Wuhan 430072, China
E-mail: jmhu@whu.edu.cn

Abstract. Pterygia, caused by fibrovascular growth of conjunctiva, are a common ophthalmic disease. However, the molecular composition of pterygium tissue has not been completely understood, and therefore the aim of this study is to investigate the spectroscopic differences between normal human bulbar conjunctiva and human pterygium tissue using a confocal Raman system. The high signal-to-noise ratio spectra from pterygium and conjunctiva tissue were obtained by this technique without any sample preparation and the time of detection required less than 3 min. Comparing Raman spectra of two types of tissue, there are obvious changes, including intensity decrease at $\sim 1585\text{ cm}^{-1}$ and intensity increase at ~ 1748 , 1156 , and 1521 cm^{-1} with the lesion of conjunctiva. Additionally, the amide I vibrational mode of proteins in conjunctiva is significantly different than that in pterygium. The use of pathology, immunology, and the peroxidation of the lipids in conjunction with the Raman results indicate that the presence of additional elastic fibers, mast cells, and lymphocytes in pterygium, as compared with normal bulbar conjunctiva, have fewer unsaturated fat acids. The present study demonstrates that Raman spectroscopy can be potentially applied to diagnose pterygia clinically. © 2005 Society of Photo-Optical Instrumentation Engineers.

[DOI: 10.1117/1.1888345]

Keywords: Raman scattering; pterygium; bulbar conjunctiva; in-vitro detection.

Paper 04142 received Jul. 26, 2004; revised manuscript received Oct. 16, 2004; accepted for publication Nov. 2, 2004; published online Apr. 13, 2005.

1 Introduction

A pterygium is the most obvious ophthalmic disease and is characterized by growth of the conjunctiva. It commonly encroaches onto the cornea as a triangular or wing shape (Fig. 1). Pterygia are usually small and relatively benign, but cause considerable irritation and often recur after surgery. A proportion of cases appear to be inherited,¹ but other factors—including dust, wind, heat, infection, inflammation, and sunlight—have been proposed as causes. Nevertheless, the pathogenesis of pterygium remains unclear.

While there are still no defined causes for pterygium formation, some techniques including ultra-structural pathology,^{2,3} immunology,⁴ and the peroxidation of the lipids⁵ are used to characterize the differences of microstructure, compositions, and metabolism between the pterygium and normal bulbar conjunctiva tissue. Among these techniques, ultrastructural pathology, such as transmission electron microscope (TEM), could only provide the ultra-structure of tissue but was limited to describe the molecular composition of tissues directly. Furthermore, neither immunohistochemical staining nor peroxidation of the lipids could identify the composition of biomedical tissues with elaborate information about molecules.

Raman spectroscopy (RS) permits accurate, rapid, nondestructive, and noninvasive identification of tissues. The finger-

print spectral region, from 600 to 1800 cm^{-1} , contains a series of sharp bands that can be used to characterize a particular molecule and in some cases to identify the composition of complex tissue's samples. Since Yu et al. first introduced the application of RS in ophthalmology in 1975,⁶ investigations have focused on RS characterization of the cornea,⁷ the aqueous humor,⁸ the vitreous,⁹ and the retinal pigment.^{10–12} Up to now, no published papers involve RS characterization of human pterygium tissue.

To characterize the molecular composition of pterygium and normal bulbar conjunctiva tissues and confirm the results of ultra-structural pathology, immunology, and peroxidation of lipids, Raman spectra of pterygium and normal bulbar conjunctiva tissue, which were obtained by employing visible excitations, as well as preliminary discussions of Raman scattering properties of pterygium in conjunction with results of correlative studies, are first reported here.

2 Materials and Method

2.1 Ethical Approval

This protocol was approved by the relevant Local Research Ethics Committees (China).

2.2 Sample Preparation

Surgical specimens of pterygia and normal conjunctival specimens from age-matched pterygia patients were obtained from Wuhan AIER Eye Hospital, Wuhan, China. Written informed

Address all correspondence to Jiming Hu, Wuhan University, College of Chemistry and Molecular Sciences, Wuhan 430072, China. E-mail: jmhu@whu.edu.cn

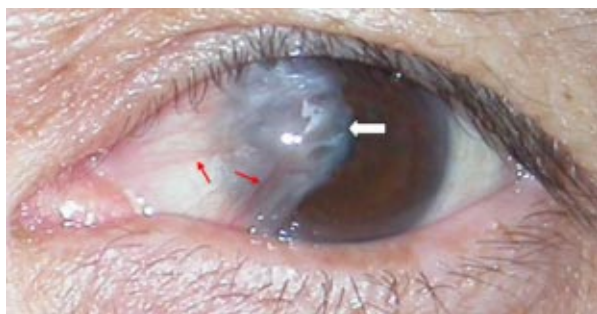


Fig. 1 Photograph of eye suffering from pterygium (taken by Nikon COOPIX 4500). The wing-shaped hyperplastic conjunctiva, which contains abundant blood vessels (red arrow), is encroaching onto the cornea (white arrow).

consent was obtained from all patients. Specimens from the patients, which included 7 women and 13 men treated for pterygia, were separated into two parts. One was used for a histochemical H&E stain (Fig. 2), and the other one was used for a frozen section. Cryosections ($25\ \mu\text{m}$ in thickness) were obtained from the biopsy specimens and placed on a gold sheet for measurement of Raman spectroscopy. There were no extra Raman peaks for the gold sheet in the fingerprint spectral region, from 600 to $1800\ \text{cm}^{-1}$ with somewhat low noise at the excitation wavelength of $514.5\ \text{nm}$. During measurement, the conjunctiva tissue section was thawed to reach room temperature and allowed to dry in air and discarded after use.

2.3 Raman Instrumentation

A Renishaw Raman microspectrometer (System RM1000, Renishaw, Wotton under Edge, U.K.), similar to the system used by Puppels et al.,¹³ was optimized for maximum throughput, detection sensitivity, and fluorescence suppression. The argon ion laser (Spectra Physics, Mountain View, California) provided a 20-mW excitation light at $514.5\ \text{nm}$. After attenuation through prisms and filters, the power of the laser exposed on the samples was only about $4\ \text{mW}$, which makes it almost impossible for the laser to lead to degradation of the tissues. Spectra were measured from tissues with a $20\times$ short-working-distance objective (NA 0.40), and the signal was integrated for 30 to 120 seconds and measured over a spectral range of 600 to $1800\ \text{cm}^{-1}$ with respect to the excitation frequency. The system included a stigmatic spectrometer with two motorized gratings, of which the 1800 grooves/mm grating was used to provide a spectral resolution of the Raman scatter of about $5\ \text{cm}^{-1}$. Raman scattering was

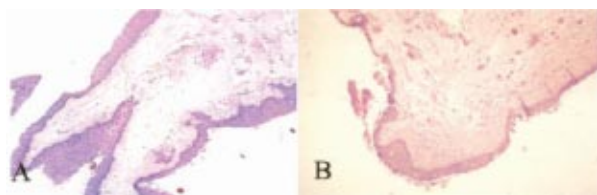


Fig. 2 Histological studies of pterygium. (A) H&E stain of pterygium showing prominent subepithelial connective tissue in the pterygium (original magnification, $100\times$). (B) H&E stain of normal conjunctiva (original magnification, $100\times$).

detected by using an air-cooled 578×385 -pixel CCD camera. Peak frequencies and rapid checking of instrumental performance were calibrated with the silicon phonon line at $520\ \text{cm}^{-1}$. Spectral data were visualized on a computer and processed for baseline correction and normalization by the GRAMS/32 spectroscopic software (Thermo Galactic). Profile data were then imported into Origin 7.0 software (Origin Lab Corporation).

3 Results

The confocal Raman system (CRS) technique yielded rapid acquisition of high-SNR Raman spectra of the human normal bulbar conjunctiva and pterygium tissue using 514.5-nm laser irradiation. Typical Raman spectra obtained from normal bulbar conjunctiva (a) and pterygium (b) tissue, without any sample preparation, are shown in Fig. 3. The inset in Fig. 3 shows the spectra of the above-mentioned tissue before background subtraction.

The CRS as presented here has various advantageous properties, as mentioned in many reports.¹³ The high gain of this optical system design is the high numerical aperture objective lens and a highly sensitive CCD camera. The confocal arrangement prevents the detection of stray light and enables the probing of small optical volumes, yielding adequate spatial resolution. To minimize the auto-fluorescence of tissues under visible excitation, the CRS should be optimized by reducing the slit and CCD area to suppress fluorescence and get high performance. Furthermore, laser bleaching was often employed, which means most samples should be irradiated by laser about 1 min to minimize its auto-fluorescence. This system had the highest spatial and spectral resolution; the laser was focused to a small spot within the sample and the Raman scattered light collected only from that point.¹³ Theoretically, the size of laser spot in our experiments could be given by $s = 0.61 \cdot \lambda / \text{NA}$, and it was about $0.8\ \mu\text{m}$. Factually, the laser beam was focused manually on individually spots by means of a microscope objective to a spot of 1 to $2\ \mu\text{m}$ in diameter. The power density was generally defined as the ratio of the power of the laser to the area of the spot, which means power density here was about $1\ \text{mw}/\mu\text{m}^2$. Therefore, the spectra that were collected with such low excitation powers did not reveal changes that could be attributed to tissue heating.¹⁴

The main Raman bands and their assignments are listed in Table 1. The primary Raman peaks of tissue were observed at 1003 , 1172 , 1306 , 1362 , 1395 , 1585 , and $1639\ \text{cm}^{-1}$, etc., presented in both tissue samples except for the bands at 1156 , 1524 , 1656 , and $1748\ \text{cm}^{-1}$, which only appeared in the spectra of pterygium. Additionally, the Raman band appears at $\sim 1450\ \text{cm}^{-1}$ in the spectra of bulbar conjunctiva but at $\sim 1440\ \text{cm}^{-1}$ in that of pterygium, which should be assigned to $\text{CH}_3(\text{CH}_2)$ deformation vibration of proteins.

Raman bands of tissues, including the bulbar conjunctiva and pterygium tissue, result primarily from protein vibrations, such as amide I at ~ 1656 and $1639\ \text{cm}^{-1}$, amide III in the 1220 to 1300-cm^{-1} region,¹⁵ CH_2 (or CH_3) deformation vibration of protein at $\sim 1450\ \text{cm}^{-1}$,¹⁶ and CH_2 twisting and wagging vibration at 1306 and $1172\ \text{cm}^{-1}$.¹⁷ Furthermore, there are more specific Raman scattering for smaller molecular compounds, such as the very characteristic sharp band for ring-breathing vibration of phenylalanine at $\sim 1003\ \text{cm}^{-1}$,

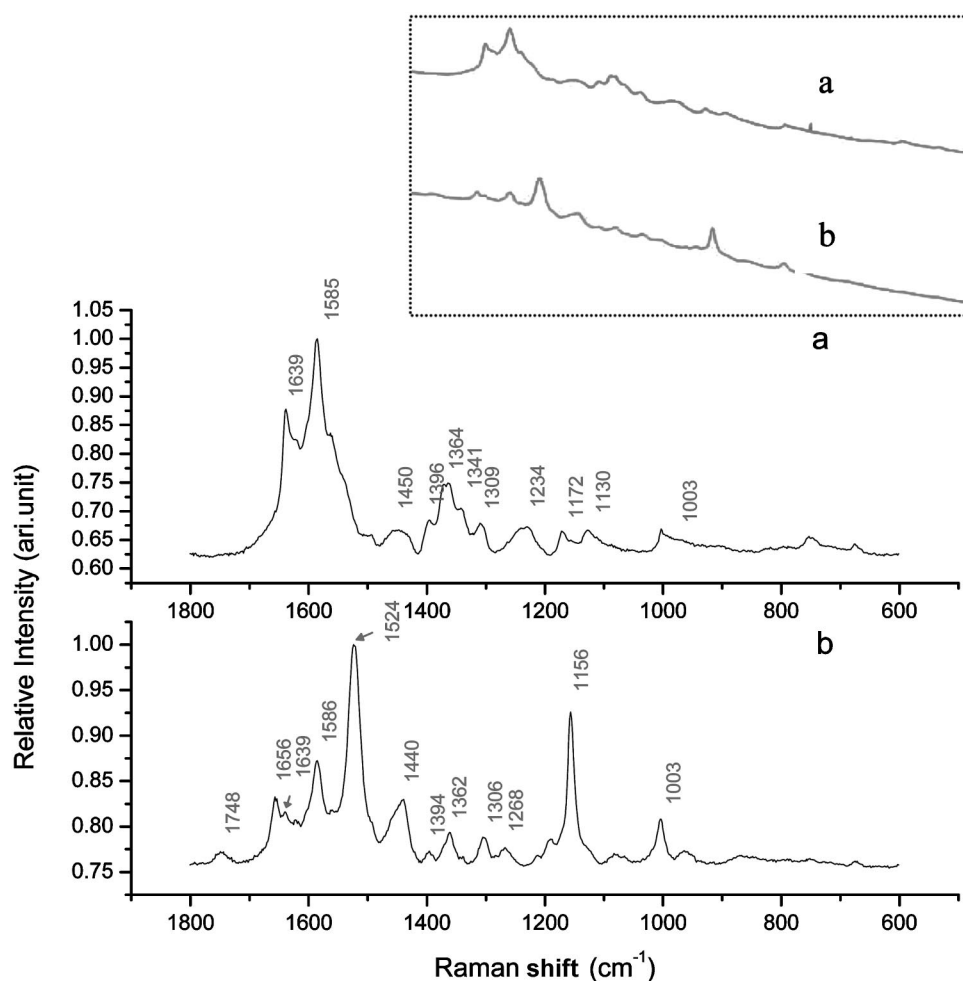


Fig. 3 Raman spectra of (a) normal human bulbar conjunctiva and (b) human pterygium in the 600- to 1800- cm^{-1} region with 3-min acquisitions and baseline subtraction. The corresponding spectra before baseline subtraction are inserted in the figure.

which appears in all protein-containing samples. On the other hand, vibration of lipids also appears in the spectra of two types of tissue, such as the band at $\sim 1585 \text{ cm}^{-1}$, which should be assigned to the stretching vibration of C=C in unsaturated fat acids, and the band at 1364 cm^{-1} , which may be assigned to CH_3 symmetrical deformation vibration of lipids.¹⁷

4 Discussion

Figure 3 depicts the typical Raman spectra of normal bulbar conjunctiva [Fig. 3(a)] and pterygium [Fig. 3(b)] tissues in the range of Raman shift from 600 to 1800 cm^{-1} . Even at an exposure time of less than 3 min, the SNR is sufficiently clear to distinguish the pterygium from normal bulbar conjunctiva.

4.1 Elastic Fibers: The Main Composition of Pterygium

The connective tissues are generally composed of elastic fibers and collagenous fibers, and these two typical fibers are mainly made up of elastin and collagen, respectively. Accumulation of elastin in solar elastosis in photodamaged skin

Table 1 Raman band position and tentative assignment of pterygium and normal human bulbar conjunctiva tissues.

Raman band position (cm^{-1})	Assignments ¹⁵⁻¹⁷
1748	"C=O" stretching vibration
1656	amide I of elastin
1640	amide I of collagen
1585	"C=C" olefinic stretching of lipids
1524	"-C=C-" stretching of carotenoid
1450/1440	d $\text{CH}_2(\text{CH}_3)$
1364	CH_3 symmetrical deformation vibration of lipids
1306/1172	CH_2 twisting and wagging
1220-1250	amide III
1156	"-C-C-" stretching of carotenoid
1005	phenylalanine

has been demonstrated in transgenic mice, by both immunohistochemistry and molecular biology techniques.^{18–20} It is likely that the pathological changes in conjunctiva in response to chronic UV irradiation are similar to those in chronically sun-damaged skin.

The results of pathological ultra-structure of pterygium stressed that multiplication and degeneration of elastic and collagenous fibers are the prominent pathological changes, and the pre-elastic fibers and denatured elastic fibers are the main compositions of pterygium.^{2,3} Comparing the spectra of normal conjunctiva and pterygium tissue as shown in Fig. 3, there are obvious differences in the region of amide I. The bands near 1639 cm^{-1} and 1656 cm^{-1} , which should be assigned to amide I vibration of collagen and elastin, respectively, both appear in the spectra of pterygium tissue. However, only the band at 1639 cm^{-1} appears in the spectra of normal bulbar conjunctiva tissue and even its relative intensity is higher than that in the spectra of pterygium. It is demonstrated that elastin is the main type of tissue in pterygium and there are also small amount of collagen in it, which is consistent with the results of ultrastructural pathology.^{2,3}

4.2 Lymphocyte: Significant Increase in Pterygium

Several investigators have noted an increase of mast cell (MC), lymphocyte, and plasma cell numbers in pterygium.^{4,21,22} This study demonstrates the validity of these results in that there are significant increases of lymphocyte in pterygium.

Carotenoids are widely spread in all sorts of organ tissues especially in lymphocyte, and lymphocyte may be the main carrier of carotenoids in pterygium. There are two characteristic bands at $\sim 1521\text{ cm}^{-1}$ and $\sim 1156\text{ cm}^{-1}$ of carotenoids, which should be assigned to carbon-carbon double-bond stretch vibrations of the molecule's backbone and carbon-carbon single-bond stretch vibrations of carotenoids, respectively.²³ Carotenoids are π -electron conjugated carbon-chain molecules ($\text{C}_{40}\text{H}_{56}$) and are similar to polyenes in their structure and optical properties. Because of the molecular structure of polyene molecules, they elicit very strong Raman scattering, especially when resonantly excited in their π - π^* electronic absorption transition in the visible (violet/green) wavelength range.²⁴

In comparison with the spectra of normal bulbar conjunctiva tissue, typical characteristic Raman bands of carotenoids were observed only in the spectra of pterygium as shown in Fig. 3(b). This result proves that the content of carotenoids is more in pterygium tissue than in normal tissue. According to the results of immunology,^{21,22} it may be concluded that the pathological changes in pterygium tissue indicate a chronic inflammatory condition with fibrosis, and lymphocytes are thus presumed to have an important role in the pathogenesis of pterygium tissue.

4.3 Unsaturated Fatty Acids: Significant Decrease in Pterygium

Human tissues, especially for biomembrane (including cell membrane and organelle membrane), contain abundant unsaturated fatty acids. Light could induce a lipid peroxidation chain reaction of unsaturated fatty acids in limbus cornea's histiocytes. The end products of a lipid peroxidation reaction

are small molecule compounds, such as aldehyde and ketone, etc. Malondialdehyde is one of the end products of lipid peroxidation reaction and is a marker of lipid peroxidation reaction. The study of lipid peroxidation reaction stressed that the concentration of malondialdehyde in the pathologic samples was much higher than that in the normal samples ($P < 0.01$).⁵

From Fig. 3, the Raman band near $\sim 1585\text{ cm}^{-1}$ should be assigned to a C=C unsaturated fatty acids stretch of lipids in the pterygium tissue. It was obviously lower than that in normal bulbar conjunctiva tissue. Accordingly, the Raman band near $\sim 1748\text{ cm}^{-1}$, which should be ascribed to a C=O stretch of aldehyde or ketone, only appears in the spectra of the pterygium tissue. These results sufficiently confirm that there are significant decreases of unsaturated fatty acids in pterygium as a result of a lipid peroxidation reaction but a significant increase of malondialdehyde accordingly.

Since the late 1970s, there has been an increasing flow of articles on applied Raman spectroscopy in ophthalmology. This increase reflects the expectation that this valuable technique will be introduced in the future into clinical practice. However, to introduce the Raman technique as a clinically applied diagnostic tool, much more work has to be done. The discrepancy between system sensitivity and eye safety is the main drawback of the RS system for ophthalmic use, which still needs to be overcome to allow the safe clinical application of this optical technique for the noninvasive assessment of conjunctiva in vivo. However, we believe that with adequate improvement in system safety, RS could potentially be applied as a noninvasive tool for the assessment of conjunctiva in vivo with clinical relevance for the early diagnosis of pterygium.

5 Conclusions

This study has demonstrated the facility of confocal Raman microspectroscopy to distinguish between pterygium and normal bulbar conjunctiva tissue and the great potential of Raman spectroscopy in combination with optical fiber probes for rapidly investigating the pathology of pterygium in vivo. In conjunction with the results of ultrastructural pathology, immunology, and the peroxidation of the lipids, pterygium were discovered that had more elastic fibers, mast cells, and lymphocytes, but fewer unsaturated fat acids than normal bulbar conjunctiva tissue. We also found that elastic fibers were the main component of pterygium.

Acknowledgments

The authors gratefully acknowledge all the staff in the Wuhan AIER Eye Hospital for their generous cooperation. This project was supported by the National Natural Science Foundation of China (No. 20405011, No. 20427002, and No. 20375029) and the Natural Science Fund of Hubei Province.

References

1. F. Hecht and M. G. Shoptaugh, "Winglets of the eye: dominant transmission of early adult pterygium of the conjunctiva," *J. Med. Genet.* **27**, 392–394 (1990).
2. P. Austin, F. A. Jackobiec, and T. Iwamoto, "Elastodysplasia and elasto-dystrophy as the pathologic bases of ocular pterygia and pinguecula," *Ophthalmology* **90**, 96–101 (1988).
3. G. X. Xu, L. Y. Zhou, Y. Tong, P. Liang, F. S. Lin, and L. Y. Chen,

- "Pathological ultrastructure study of pterygium," *Chin. J. Ophthalmol.* **32**, 438–440 (1996).
4. L. Liu and D. Yang, "Immunological studies on the pathogenesis of pterygium," *Chin. Med. Sci. J.* **8**, 84–88 (1993).
 5. L. Lv, R. G. Wang, X. H. Song, H. Li, D. S. Dong, and L. H. Zou, "Pterygium and lipid peroxidation," *Chung Hua Yen Ko Tsa Chih* **32**, 227–229 (1996).
 6. N. T. Yu and E. J. East, "Laser Raman spectroscopic studies of ocular lens and its isolated protein fractions," *J. Biol. Chem.* **250**, 2196–2202 (1975).
 7. D. C. W. Siew, G. M. Clover, R. P. Coonet, and P. M. Wiggins, "Micro-Raman spectroscopy study of organ cultured corneae," *J. Raman Spectrosc.* **26**, 3–8 (1995).
 8. R. J. Erckens, M. Motamedi, J. P. Wicksted, and W. F. March, "Raman spectroscopy for non-invasive characterization of ocular tissue: potential for detection of biological molecules," *J. Raman Spectrosc.* **28**, 293–299 (1997).
 9. J. Sebag, S. Nie, K. Reiser, M. A. Charles, and N. T. Yu, "Raman spectroscopy of human vitreous in proliferative diabetic retinopathy," *Invest. Ophthalmol. Visual Sci.* **35**, 2976–2980 (1994).
 10. L. Huang, H. Deng, and Y. Koutalos, "A resonance Raman study of the C=C stretch modes in bovine and octopus visual pigments with isotopically labeled retinal chromophores," *Photochem. Photobiol.* **66**, 747–754 (1997).
 11. D. Zhao, S. W. Wintch, W. Gellermann, and P. S. Bernstein, "Resonance Raman spectroscopic measurement of macular carotenoid pigments in patients with choroidal and retinal dystrophies," *Invest. Ophthalmol. Visual Sci.* **43**, U598–U598 2544 (2002).
 12. D. Zhao, S. W. Wintch, W. Gellermann, and P. S. Bernstein, "Resonance Raman measurement of macular carotenoids in retinal, choroidal, and macular dystrophies," *Arch. Ophthalmol. (Chicago)* **121**, 967–972 (2003).
 13. K. Maquelin, L. P. Choo-Smith, T. van Vreeswijk, H. P. Endtz, B. Smith, R. Bennett, H. A. Bruining, and G. J. Puppels, "Raman spectroscopic method for identification of clinically relevant microorganisms growing on solid culture medium," *Anal. Chem.* **72**, 12–19 (2000).
 14. M. G. Shim and B. C. Wilson, "The effect of ex vivo handling procedures on the near-infrared Raman spectra of normal mammalian tissues," *Photochem. Photobiol.* **63**, 662–671 (1996).
 15. M. J. Anita and R. K. Rebecca, "Raman spectroscopy for the detection of cancers and precancers," *J. Biomed. Opt.* **1**, 31–70 (1996).
 16. M. G. Shim and B. C. Wilson, "The effect of ex vivo handling procedures on the near-infrared Raman spectra of normal mammalian tissues," *Photochem. Photobiol.* **63**, 662–671 (1996).
 17. J. M. Chalmers and P. R. Griffiths, "Handbook of vibrational spectroscopy: theory and instrumentation," Chap. 5 in *Application in Life, Pharmaceutical and Natural Sciences*, pp. 3426–3447, John Wiley & Sons, Chichester (2002).
 18. E. F. Bernstein, D. B. Brown, F. Urbach, D. Forbes, M. Del Monaco, M. Wu, S. D. Katchman, and J. Uitto, "Ultraviolet radiation activates the human elastin promoter in transgenic mice: a novel in vivo in vitro model of cutaneous photoaging," *J. Invest. Dermatol.* **105**, 269–273 (1995).
 19. W. Montagna, S. Kirchner, and K. Carlisle, "Histology of sun-damaged skin," *J. Am. Acad. Dermatol.* **21**, 907–918 (1989).
 20. J. Uitto and A. M. Christiano, "Elastic fiber," Vol. 1, *Dermatology in General Medicine*, pp. 339–349, McGraw-Hill, New York (1993).
 21. S. Okisaka, M. Kudo, M. Funahashi, and S. Nakada, "The pathogenesis of pterygium," *Ophthalmology* **27**, 633–642 (1985).
 22. Y. Kadota, "Morphological study on the pathogenesis of pterygium," *Nippon Ganka Gakkai Zasshi* **91**, 324–334 (1987).
 23. W. Gellermann, M. Sharifzadeh, M. Ermakova, and I. V. Ermakov, "Resonant Raman detectors for noninvasive assessment of carotenoid antioxidants in human tissue," *Proc. SPIE* **4958**, 78–87 (2003).
 24. S. Arikian, H. S. Sands, R. G. Rodway, and D. N. Batchelder, "Raman spectroscopy and imaging of β -carotene in live corpus luteum cells," *Anim. Reprod. Sci.* **71**, 249–266 (2002).